Influence of Aggregate Shape and Exciton Location on Polarization Energy of Benzene and Anthracene Aggregates

Thomas T. Testoff and Lichang Wang*
School of Chemical and Biomolecular Sciences
Southern Illinois University Carbondale, Carbondale, IL 62901, USA

Abstract

To investigate the aggregate shape and exciton location on the polarization energies of benzene and anthracene aggregates, we performed calculations on the clusters in increasing size and differing shape. The results showed that the anthracene cluster showed no apparent difference in the shape dependence, however, benzene clusters differed significantly due to its nearest neighbors orient in a T-shape conformation compared to anthracene which is more stacked along its conjugated rings. Additionally, lower total energies of the 'full' model as well as less stable neutral energies for the surface molecules in the 'intra+inter' model suggest that the surface molecules interact repulsively. Due to the fact that the cube structure has a larger surface area to volume ratio and more benzene molecules are needed to take up said surface area more repulsive force may be experienced by molecules in the benzene cubes. Apparent polarization energy of each system increases as number of close by neighbors increases. Therefore molecules located centrally have larger induced dipole polarization as well as larger apparent polarization. Apparent polarization energy depends more sensitively on the location of the excitation than the shape of the cluster. Furthermore, the orientation of the nearest neighbors in each direction plays a large role in magnitude of the electrostatic interactions as well as the induced dipole effects.

* Corresponding author: lwang@chem.siu.edu

1. Introduction

The effect of aggregation on the electronic properties of organic small molecule (OSM) based solids on material performance is well known,[1-3] however, specific and measured changes in the properties such as UV-Vis absorption caused by aggregation of OSMs due to long range columbic interactions are not fully predicted but are urgently needed in order to rationally design OSM based devices, such as solar cells[4-27] and sensors,[28-54] as well as to better utilize aggregation phenomenon. Extensive studies of single molecule of OSM based materials on the property [55-95] and synthesis [96-133] can be found, in contrast to, investigations on aggregation of OSMs have just become an active research field.[1-3,134-168]

The change in the properties of aggregates such as in UV spectra is due to the change in band structure upon aggregation, the edge of which determines the lowest energy needed to excite electrons and thus the extent of the red-shift. The change of this band edge energy is also directly related to the change in the ionization potential and electron affinity through Koopman's theorem and the apparent polarization energy. Specifically, changes in the IP and EA due to the apparent polarization can be taken as the change in the HOMO and LUMO energy to that of the band edge. As such, the excitonic energy splitting that creates the new band edge can be approximated by calculating the apparent polarization due to anionic and cationic molecules in the aggregates.

While the excitonic energy splitting can be somewhat characterized using the point-dipole approximation of the Kasha Model, explicit calculation of systems based upon the density functional theory (DFT) or ab initio quantum mechanical (QM) approaches are limited. Particularly, when molecular systems are amorphous, on the size of nanometers, or a measure of disorder is introduced (defects, etc.). Outside of QM approaches and DFT which rely on accurate functionals, lack scalability for disordered systems, and often need to utilize some type of basis set

superposition correction; three types of methods have come to the fore including QM/MM, field model representations, and polarizable force fields.

Each of these methods have their own strengths in weaknesses. Field models are extremely scalable and accurate for crystalline structures, but their inability to account for differences in molecular packing and small electrostatic differences make them unsuitable for many models. QM/MM explicitly treats a portion of the local molecular model and allows for direct extrapolation of bulk properties, but has been found to overestimate the polarization energy and is more costly than a classical approach. Additionally, QM/MM models must make decisions as to what portion of the system will be treated explicitly by QM methods. Last is the classical force fields who have a knack for being able to treat non-repeating structures at the nanoscale, and scalability allows for them to be used for amorphous bulk rather easy. The main drawback is that force fields are only tangentially related to the QM calculated properties through parameterization.

Polarizable force fields have explicit terms to represent the electrostatic interactions between molecules, including multipole interactions and induced dipole interactions. The AMOEBA force field has been utilized by Xu et al. and others to extrapolate changes in the IP and EA of bulk oligoacenes. Xu et al. has shown that the isotropic atomic polarizability parameterized by the method put forward by Ren to be quantitatively different for anions, molecules with extended conjugation, and extremely electronegative atoms in organic aromatics. The introduction of state specific atomic polarizabilities (SSAPs) has allowed for parameterization that is specific for each atomic conformation. SSAPs utilize the single molecule electron density and the quantum theory of atoms in molecules (QTAIM) by Bader to calculate the change in the atomic multipole moments under a minute field. The change in the multipole moments due to the field directly show the susceptibility of the electron density around each atom to fields produced by other molecules.

Herein, Ren's parameterization procedure is combined with SSAP parameterization to respectively produce the atomic multipole moments (AMPs) and the isotropic atomic polarizability of benzene and anthracene. The explicit polarization terms are utilized to calculate the apparent polarization energy of clusters of increasing size. Using this polarizable force field model, we developed parameters for benzene and anthracene aggregates and calculated the polarization energy of various spherical aggregates.[169]

The objectives of this work is twofold. Firstly, in the interest of looking at non-bulk nanostructures, cube shaped benzene and anthracene aggregates were studied in this work so that the effect of cluster shape on the polarization energy of aggregates can be explored. Specifically, properties of a cube cluster was compared to the spherical cluster at the same size. Secondly, exciton location was placed at the center as well as the surface of aggregates so that the effect of exciton location on the polarization energy can be investigated. Specifically, a total of 6 cubed anthracene aggregates and 7 cubed benzene aggregates with four different excitations, i.e. center, surface, corner, and ridge were studied. Furthermore, 9 spherical benzene aggregates and 10 spherical anthracene aggregates with surface excitation were also studied here.

2. Computational Details

The cube clusters of benzene and anthracene were created using the Materials studio based on the experimentally determined XRD structures of the corresponding crystals in the similar fashion as the corresponding spherical clusters.[169] Apparent polarization energy (W) was calculated using Eq.(1) that arises from three main terms within the AMOEBA force field as described previously by Xu,[170] ourselves,[169] and others. Each term is the differential energy between the change in the bulk ionic energy from that of the single ion and that of the neutral bulk

system and the neutral molecule Eq. (2). As dispersion has not been specifically parameterized by changing the potential well depth nor will the cluster geometry change between the neutral and ionic system, equation one simplifies to the sum of the first two terms. This has been shown to be a reasonable assumption as the differences in the electrostatic forces between the ionic bulk and neutral system are much larger than that of dispersion, making them insignificant unless the formation of the ion causes a relaxation and change in geometrical structure of the cluster or bulk.

$$W^{+/-} = \Delta E^{es} + \Delta E^{pol} + \Delta E^{dis} \quad \text{Eq.1}$$

$$\Delta E^{pol} = \left(E^{pol}_{bulk,ion} - E^{pol}_{gas,ion}\right) - \left(E^{pol}_{bulk,neu} - E^{pol}_{gas,neu}\right) \quad \text{Eq.2}$$

Details of the explicit terms used to describe the induced dipole polarization (P) and the electrostatic interaction can be found in the original paper's published by Ponder,[171,172] the parameterization methods for the Tinker software by Ren, the work detailing SSAP parameterization by Xu,[170] as well as briefly in our previous work. In order to ensure the fidelity of the AMOEBA force field, the TINKER 8.0 software was used. Modifications were made to the printable interactions within the software in order to sum the intermolecular interactions between the atoms of the ionic molecule and the atoms of the surrounding molecules. Additionally, the intramolecular interactions between the ionic molecule itself were taken into account. Adding the molecular interactions separately allowed for the delineation of our results into three model: the 'full' model taking into account of all interactions except intramolecular induced dipole interaction as dictated by polarization grouping in AMOEBA), the intermolecular model taking into account

solely the interactions between the atoms of the ion and its surrounding molecules atoms, and the 'intra+inter' molecular model which took into account intramolecular multipole interactions of the ionic molecule as well as the forces dictated in the 'inter' model.

AMOEBA was utilized with AMPs generated from Ren's parameterization method and isotropic atomic polarizabilities from SSAPs and QTAIM. For the AMPs single molecule structures of benzene and anthracene neutral molecules were optimized at the MP2 level using the 6-311G(d,p) basis set. Anions and Cations were then calculated at the same level using the neutral molecule geometry. As dictated in Ren's parameterization procedure GDMA2.3 was used to calculate the AMPs using the Gauss-Hermite Quadrature. For electrostatic potential fitting of AMPs benzene and anthracene neutral molecules were further optimized at the MP2/aug-cc-pvtz level. Anionic and cationic species electron density was additionally calculated using the geometry of the neutral species as before. The electrostatic potential fitting gradient was set to 0 .1.

SSAPs were generated utilizing QM calculations of the electron density of anthracene and benzene species at the CAM-B3LYP / 6-311+G(d,p) level with the optimized molecular geometry of each neutral molecule at the B3LYP / 6-31+G(d,p) level. Calculations were done for the positive, negative and neutral species of both benzene and anthracene under electric fields of 005 a.u. strength in each cartesian direction. QM electron densities were then subjected to Keith's implementation of Bader's hard-space partitioning to generate the atomic multipoles of each atom under each specific field condition in the AIMALL program. Atomic polarizability tensors were generated using symmetric numeric differentiation and the trace of the resulting matrix gave the isotropic atomic polarizability. The scalar values were then scaled by 1.4. All the parameters were obtained in our previous studies.[169]

Ionic SSAPs and AMPs were placed at the molecule nearest the COM of the Sphere and Cube Structures. Additionally, the Ionic SSAPs were placed on the central surface molecule, the central ridge molecule, and the corner molecule for the cube structure as well as on the surface of the sphere. AMOEBA calculations were then carried out at increasing clusters size. For the CTE model the cationic AMPS and SSAPs were placed at the center of the sphere and cube structures as well as the aforementioned surface positions. The anion was then assigned to the nearest neighboring molecule to the cation to create a CTE where the electron has 'hopped' to the adjacent molecule. In order to compare the CTE energy to that of its vacuum equivalent as suggested in Eq. (2), a dimer was calculated at the same orientation and intermolecular distance as in the crystal in two ways. First, both molecules were assumed to be neutral; this was the representation of the neutral system in gaseous phase. The second representation had the negative and positive SSAPs and AMPS place on the adjacent molecules in the dimer. While this system is also charge neutral, it is the representation of the CTE dimer with which to compare the bulk.

3. Results and Discussion

3.1 Effect of Aggregate Shape on Intermolecular Energy and Apparent Polarization

First considering the total energy of the neutral cluster where the energy only considers the non-bonded interactions of the aggregate (or cluster), $E = E^{es} + E^{pol} + E^{dis}$, it can be seen that for Anthracene there is no distinct difference between the cube and spherical cluster. The extrapolated bulk values are approximately -1.43 eV for the 'intra+inter' model and -2.36 eV for that of the 'inter' model. This indicates that the intramolecular energy of Anthracene is around 0.93 eV. For Benzene the electrostatic and dispersion energies indicate that the Spherical conformation is more stable than that of the cube. Specifically, the 'intermolecular energies

extrapolated from the sphere or cube shape clusters are -1.27 and 0.07 respectively. The intramolecular energy should and does remain the same at 0.44 eV. Including the surrounding molecule's interaction the total intermolecular energy per molecule is of anthracene is -0.17 eV. The benzene sphere has an intermolecular energy of -0.16 per molecule and 0.49 eV per molecule for the cube (also denoted as box in Figure 1 and the following Figures).

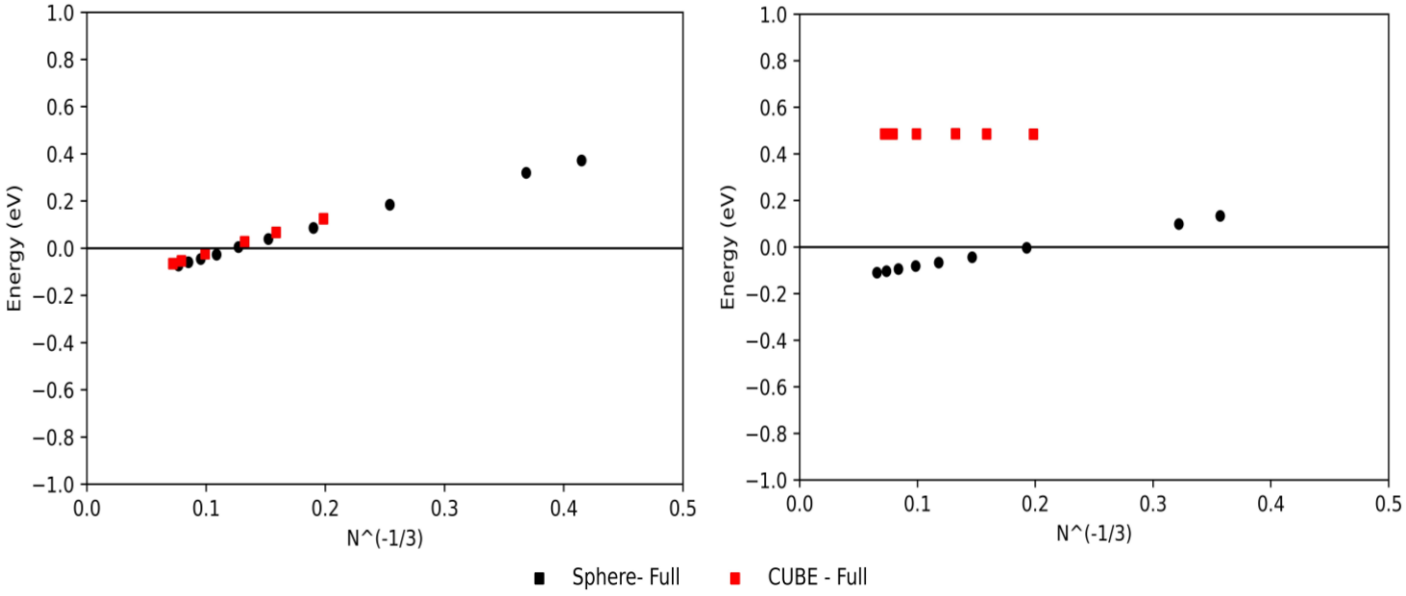

Figure 1. The total intermolecular and intramolecular energy per molecule of the anthracene (left) and benzene aggregates (right). The total energy is made up of the 14-7 dispersion interaction, electrostatic multipole interaction, and the induced dipole interaction. The data for the spherical clusters was taken from Ref. 169.

The values for the 'full' model are calculated as an average over the change in total energy. The total energy per molecule being lower as well as the more positive energies of the neutral clusters when the molecule of interaction is taken as a surface molecule indicate that as molecules are closer to the surface the intermolecular interaction becomes more repulsive. Given that the same number of the same molecules take up the same volume, perhaps the greater surface area of

the cube cluster than that of the cube increases the number of molecules exposed at the surface and therefore creates more negative interaction energies. Additionally, the exposure of the nearest neighbors of the benzene are in that of a T-Shape compared to anthracene which is more stacked along its conjugated rings. This could be reflected in greater repulsion between nearest neighbors at short range and more repulsive interactions in the long range.

Examining closely on the apparent polarization energy, it can be seen that the induced dipole polarization is more equivalent between cluster differences and that a large majority of the discrepancy arises from AMP interaction. In particular the intramolecular AMP interaction of the benzene anion depolarizes benzene, leading to lower bulk apparent polarization values. Anthracene induced dipole polarization is extremely consistent across cluster models and the apparent polarization is minutely more effected by the electrostatic multipole interactions. This leads to slightly higher Bulk HOMO values but lower Bulk LUMO values and an nearly equivalent transport gap. Looking back at benzene, consistent polarization due to the cation produces identical bulk HOMO values, but the aforementioned difference in Anion electrostatic multipole interactions causes a less stable bulk LUMO for the cube structure.

3.2 Differences in Apparent Polarization of Surface Ion between the Cube and Spherical Aggregates

Figure 2 and Figure 3 show that as the number of close proximity neighbors to the charged species increase so to does the apparent and induced dipole polarization. The only exception to this is the benzene anion cube cluster. The cube cluster stabilizes the anion through induced dipole interactions in the same manner as the other cluster shapes, charges, and molecules. That is to say that the induced dipole polarization of the bezene anionic cube cluster decreases as the number of close proximity neighbors decreases (Central >Surface>Ridge> Corner), however the electrostatic

interaction of the anion for the structures with more neighbors is much higher than that of anthracene and end up playing a more dominant role. Whereas for the other conformations across the other molecules the induced dipole polarization stabilization is anywhere from 2 to 3 times as large, for the benzene anion the ratio is closer to 1:1. Benzene anion's more consistent deviation is likely due to the larger carbon and hydrogen SSAP values, the orientation of Benzene to its nearest neighbors as well as the fact that the anion's electron density symmetry seems to be broken, resulting in larger SSAP and AMP values for two of the carbons.

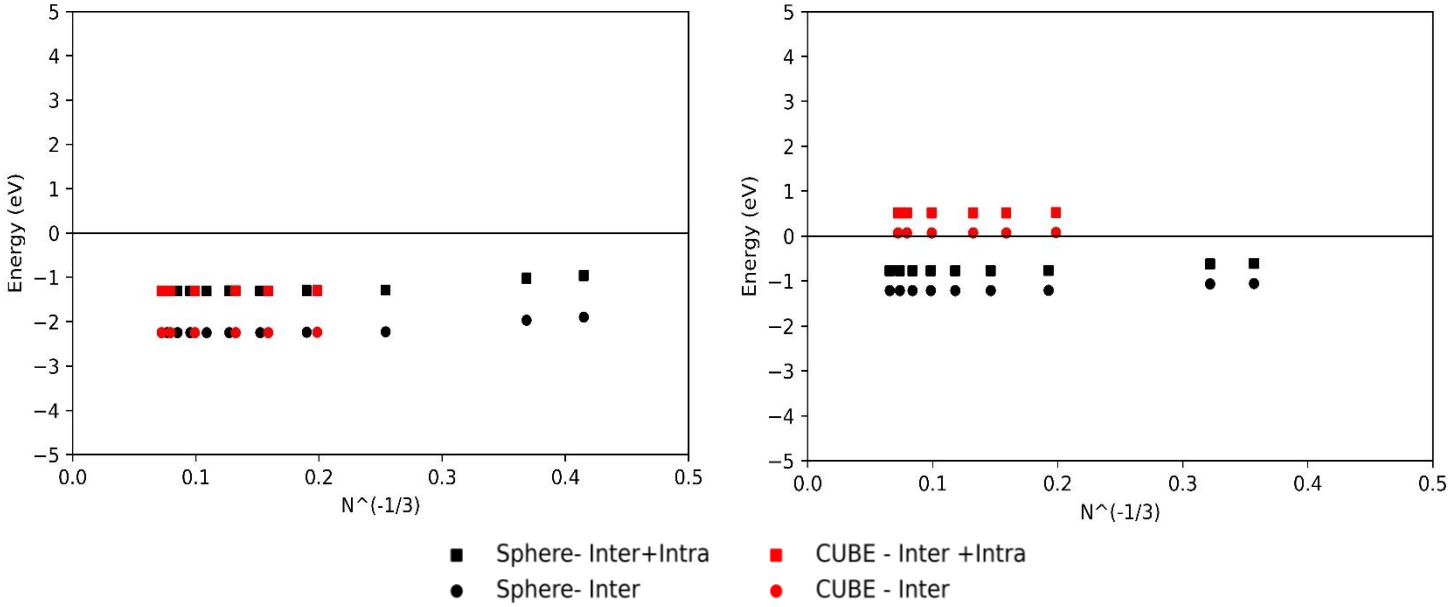

Figure 2. Total inter molecular energy between the ionic molecule and the rest of the molecules in the spherical and rectangular cluster. The intra+inter model includes the intramolecular energy of the ionic molecule. Anthracene cluster total energy is on the right and benzene is on the left. The data for the spherical clusters was taken from Ref. 169.

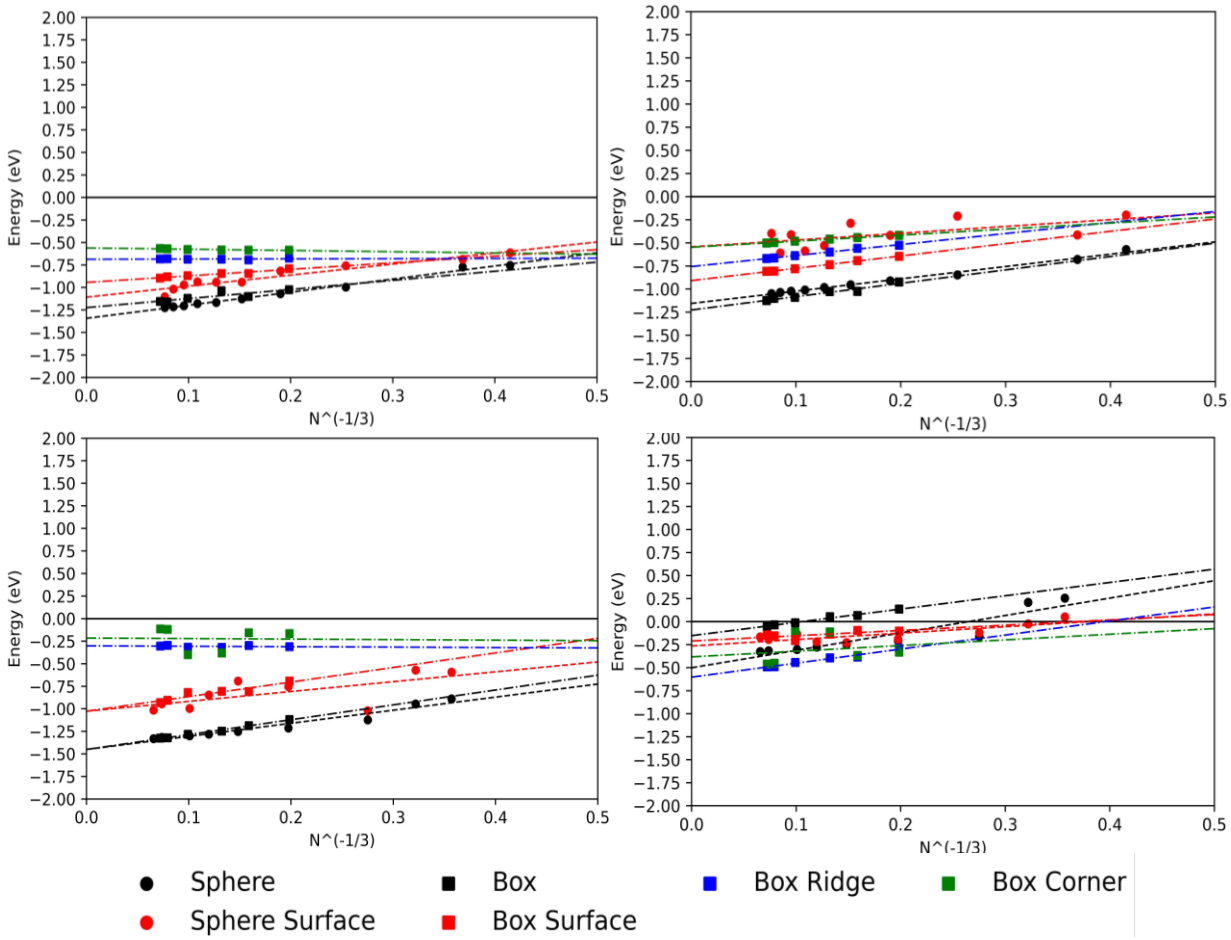

Figure 3. The apparent polarization energy of anthracene (top) and benzene (bottom) for the positive (right) and negative (left) charge carrier. The data for the spherical clusters with center charge was taken from Ref. 169.

It can also be seen that as the number of close neighbors decreases the polarization due to electrostatic multipole interaction decreases at least until the ridge molecule. For the anionic species the AMPs create are less depolarizing, whereas for the positively charge molecule in the cluster the more close proximity neighbors the smaller the polarizing effect. The reverse of this trend between the ridge and corner structures for anthracene and the benzene cation indicate that the orientation of the nearest neighbors in each direction plays a large role in magnitude of the electrostatic interactions as well as the induced dipole effects. Additionally, it indicates that each specific orientation between two molecules in the crystal structure will have a specific depolarizing or polarizing effect. For instance, all molecules stacked along the conjugated ring structure of

anthracene would be expected to have a polarizing effect, stabilizing the system, whereas the end to end stacked conformation would be expected to be depolarizing.

Decrease in the polarization due to both the positively and negatively charged molecules as the molecule comes to the surface and experience less close neighbor interactions means that the transport gap will decrease (Figure 4). This indicates that the creating a free charge carrier on the surface of a cluster and by extension the bulk solid will be increasingly more difficult. Decreased polarization of surface molecules could be a factor in the effect of film thickness on the red shift of organic thin films. The closer molecules are to the surface or smaller number of molecules within a certain radial distance causes a higher thin film band edge.

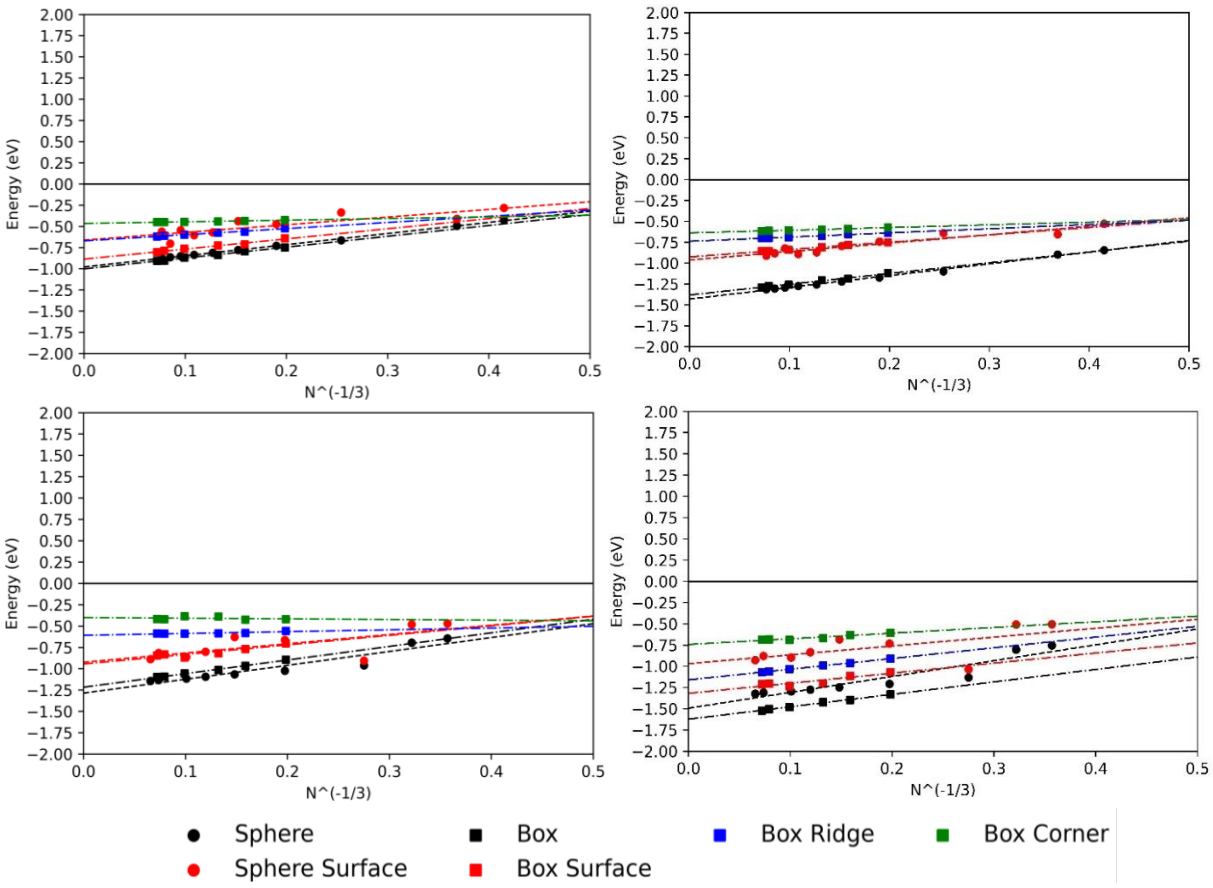

Figure 4. The difference in the apparent polarization energy of charged and neutral clusters for anthracene (top) and benzene (bottom). The positive and negative charge carrier effect on the polarization are on the right and left respectively. The data for the spherical clusters with center charge was taken from Ref. 169.

3.3 Assessment of the Charge Transfer Exciton Model

The charge transfer electron polarization can be found in Figure 5. The CTE apparent polarization follows the same pattern to the positive and negative charge carriers. Specifically, as the charge is left with fewer close neighbors the apparent polarization decreases. A cursory look at the induced dipole polarization shows this trend more clearly and a more linear relationship. This linear trend can also be seen for the apparent polarization energy of the clusters with centrally placed excitons although there are a few outlying points. There seems to be two distinct corner types of excitons for anthracene as well as different central excitons for the cube structure of benzene. The electrostatic energy further exposes these truth that these are two distinct types of exciton. While the induced dipole polarization of the system remains linear there are large differences in electrostatic energy. This energy should remain relatively constant. The small multipole moments of benzene and anthracene due to their symmetry as well as the fact that the electrostatic interaction scales inversely with the r^3 should indicate that the vast majority of the difference should be near maximum within the first 10-20 angstroms. The fact these values are so distinct is then most likely due to the orientation of the molecules that are nearest neighbors and have differing and larger than normal SSAP and AMPs values. Namely, the two molecules modeling the exciton.

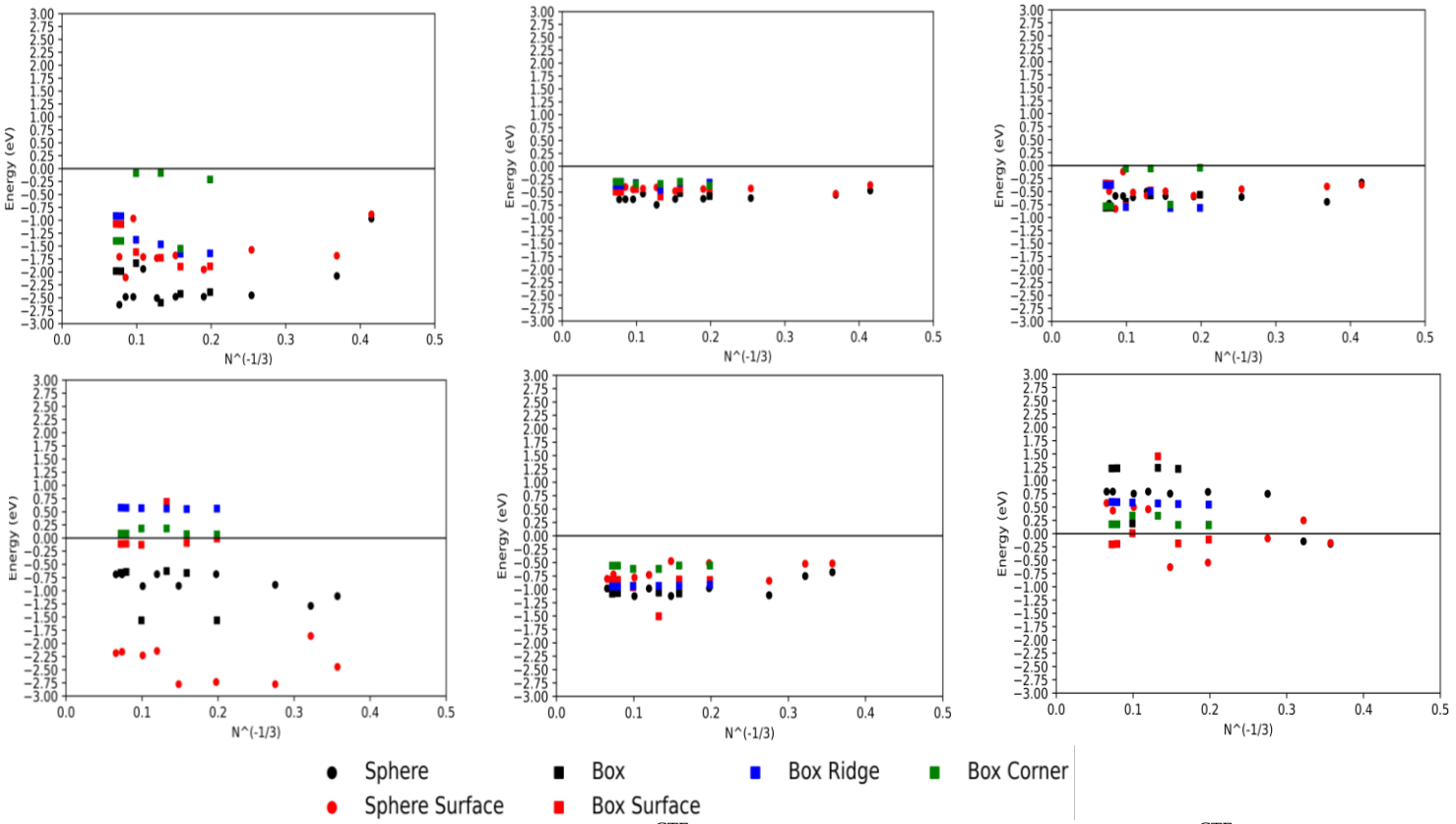

Figure 5. The apparent polarization energy (W^{CTE} - left), delta induced dipole polarization (ΔP^{CTE} -middle), and delta electrostatic energy (ΔES^{CTE} - right) of the exciton for anthracene (Top Row) and benzene (Bottom Row). The data for the spherical clusters with center charge was taken from Ref. 169.

This highlights that distinct excitons exists at different points along the spherical cluster surface, as well as the fact that the anion and cation's SSAPs and AMPs can be oriented toward another in a distinctly different way despite being the same nearest neighbor. This is likely due to the anion's symmetry breaking the benzene anion. Additionally, the slip stacking is different at the differing corners of anthracene. Care must be taken to either indicate all of the corners orientation values are being taken or that a specific corner orientation is being utilized. Additionally, orientation of symmetry broken ions must be taken into account.

4. Conclusions

Calculations were performed on the clusters of benzene and anthracene molecules in increasing size and differing shape that were generated using the experimentally determined XRD structures with ionically charged SSAPs and AMPs to central and surface molecules as well as the neutral systems to extrapolate the dependence of apparent polarizations on the cluster shape and location of excitations. The results showed that the anthracene cluster showed no difference in stability of the neutral system and consistent intramolecular energy. Benzene, however, differed significantly due to its nearest neighbors orient in a T-Shape conformation compared to anthracene which is more stacked along its conjugated rings. This could be reflected in greater repulsion between nearest neighbors at short range. Additionally, lower total energies of the 'full' model as well as less stable neutral energies for the surface molecules in the 'intra+inter' model suggest that the surface molecules interact repulsively. Due to the fact that the cube structure has a larger surface area to volume ratio and more benzene molecules are needed to take up said surface area more repulsive force may be experienced by the benzene cube model.

Apparent polarization energy of each system increases as number of close by neighbors increases. Therefore molecules located centrally have larger induced dipole polarization as well as larger apparent polarization. By extension non-surface free charge particles will have lower transport gap energies. The electrostatic energy plays a large part in the depolarization of the benzene system causing an opposite effect in the benzene anion. This change is due to the nearest neighbor interactions making a larger part of the total ES contribution to the polarization, due to their being less neighbors within a significant distance. For the anionic species the AMPs are less depolarizing, whereas for the positively charge molecule in the cluster the more close proximity neighbors the smaller the polarizing effect. The reverse of this trend between the ridge and corner

structures for anthracene and the benzene cation indicate that the orientation of the nearest neighbors in each direction plays a large role in magnitude of the electrostatic interactions as well as the induced dipole effects. Specifically each orientation between two molecules in the crystal structure will have depolarizing or polarizing effects, e.g. molecules with $\pi - \pi$ stacking would be expected to have a stabilizing effect whereas the end to end stacked conformation would destabilize. Approximations of the transport gap are relatively close to the experimental results for the centrally charged system, but rely heavily on an accurate description of the LUMO energy as well as a functional/basis set with a good description of the anion's electron density.

The CTE model can be employed with centrally charged molecules in the cluster and give relatively consistent results. Care must be taken to orient the SSAPs and AMPs toward one another in the same orientation despite being placed on the same nearest neighbor. This will not affect the induced dipole polarization, but will affect the electrostatic energy due to the multipole moments. Stacking and orientation between differing corner structures within the anthracene system give distinct differences in CTE values. All CTE energies are overestimated. They should be lower than the transport gap value and specifically around 1.0 eV for anthracene.

Acknowledgements

Thomas Testoff acknowledges the support of the Gower Fellowship and the Doctoral Research Award, Southern Illinois University Carbondale.

References

(1) Zhang, N.; Zhu, J.; An, D.; Zhang, R.; Lu, X.; Liu, Y. *Org. Lett.* **2022**, *24*, 5439.
(2) Mohajeri, A.; Farmani, M. *ACS Appl. Electron. Mater.* **2022**, *4*, 246.
(3) Xu, F.; Testoff, T. T.; Wang, L.; Zhou, X. *Molecules* **2020**, *25*, 4478.
(4) Ge, F.; Xu, F.; Gong, K.; Liu, D.; Li, W.; Wang, L.; Zhou, X. *Dyes Pigm.* **2022**, *200*, 110127.
(5) Xu, F.; Gong, K.; Liu, D.; Wang, L.; Li, W.; Zhou, X. *Solar Energy* **2022**, *240*, 157.
(6) Feng, W.; Geng, R.; Liu, D.; Wang, T.; Testoff, T. T.; Li, W.; Hu, W.; Wang, L.; Zhou, X. *Org. Electronics* **2021**, *703*, 121742.
(7) Sun, H.; Liu, D.; Wang, T.; Li, P.; Bridgmohan, C. N.; Li, W.; Lu, T.; Hu, W.; Wang, L.; Zhou, X. *Org. Electronics* **2018**, *61*, 35.
(8) Sun, H.; Liu, D.; Wang, T.; Lu, T.; Li, W.; Ren, S.; Hu, W.; Wang, L.; Zhou, X. *ACS Appl. Mater. Interfaces* **2017**, *9*, 9880.
(9) Yashwantrao, G.; Saha, S. *Dyes Pigm.* **2022**, *199*, 110093.
(10) Xu, C.; Zhao, Z.; Yang, K.; Niu, L.; Ma, X.; Zhou, Z.; Zhang, X.; Zhang, F. *J. Mater. Chem. A* **2022**, *10*, 6291.
(11) Venkatesan, S.; Hsua, T.-H.; Wong, X.-W.; Teng, H.; Lee, Y.-L. *Chem. Eng. J.* **2022**, *446*, 137349.
(12) Pettipas, R. D.; Hoff, A.; Gelfand, B. S.; Welch, G. C. *ACS Appl. Mater. Interfaces* **2022**, *14*, 3103.
(13) Koteshwar, D.; Prasanthkumar, S.; Singh, S. P.; Chowdhury, T. H.; Bedja, I.; Islam, A.; Giribabu, L. *Mater. Chem. Front.* **2022**, *6*, 580.
(14) He, S.; Lan, Z.; Zhang, B.; Gao, Y.; Shang, L.; Yue, G.; Chen, S.; Shen, Z.; Tan, F.; Wu, J. *ACS Appl. Mater. Interfaces* **2022**, *14*, 43576.
(15) Ni, M.-Y.; Leng, S.-F.; Liu, H.; Yang, Y.-K.; Li, Q.-H.; Sheng, C.-Q.; Lu, X.; Liu, F.; Wan, J.-H. *J. Mater. Chem. C* **2021**, *9*, 3826.
(16) Munoz-Garcia, A. B.; Benesperi, I.; Boschloo, G.; Concepcion, J. J.; Delcamp, J. H.; Gibson, E. A.; Meyer, G. J.; Pavone, M.; Pettersson, H.; Hagfeldt, A.; Freitag, M. *Chem. Soc. Rev.* **2021**, *50*, 12450.
(17) Kokkonen, M.; Talebi, P.; Zhou, J.; Asgari, S.; Soomro, S. A.; Elsehrawy, F.; Halme, J.; Ahmad, S.; Hagfeldt, A.; Hashmi, S. G. *J. Mater. Chem. A* **2021**, *9*, 10527.
(18) Sil, M. C.; Chen, L.-S.; Lai, C.-W.; Chang, C.-C.; Chen, C.-M. *J. Mater. Chem. C* **2020**, *8*, 11407.
(19) Mariotti, N.; Bonomo, M.; Fagiolari, L.; Barbero, N.; Gerbaldi, C.; Bella, F.; Barolo, C. *Green Chem.* **2020**, *22*, 7168.
(20) Huaulmé, Q.; Mwalukuku, V. M.; Joly, D.; Liotier, J.; Kervella, Y.; Maldivi, P.; Narbey, S.; Oswald, F.; Riquelme, A. J.; Anta, J. A.; Demadrille, R. *Nat. Energy* **2020**, *5*, 468.
(21) Wen, X.; Nowak-Krll, A.; Nagler, O.; Kraus, F.; Zhu, N.; Zheng, N.; Mgller, M.; Schmidt, D.; Xie, Z.; Wurthner, F. *Angew. Chem. Int. Ed.* **2019**, *58*, 13051
(22) He, X.; Yin, L.; Li, Y. *J. Mater. Chem. C* **2019**, *7*, 2487.
(23) Manfredi, N.; Trifiletti, V.; Melchiorre, F.; Giannotta, G.; Biagini, P.; Abbotto, A. *New J. Chem.* **2018**, *42*, 9281.
(24) Zhang, L.; Cole, J. M. *J. Mater. Chem. A* **2017**, *5*, 19541.
(25) Wang, T.; Sun, H.; Zhang, L.; Colley, N. D.; Bridgmohan, C. N.; Liu, D.; Hu, W.; Li, W.; Zhou, X.; Wang, L. *Dyes Pigm.* **2017**, *139*, 601.
(26) Gong, J.; Sumathy, K.; Qiao, Q.; Zhou, Z. *Renew. Sust. Energy Rev.* **2017**, *68*, 234.
(27) Ding, G.; Tang, A.; Chen, F.; Tajima, K.; Xiao, B.; Zhou, E. *RSC Adv.* **2017**, *7*, 13749.
(28) Chen, Z.; Yang, L.; Xu, W.; Xu, F.; Sheng, J.; Xiao, Q.; Song, X.; Chen, W. *Anal. Chem.* **2023**, *95*, 3325.

(29) Feng, W.; Zengji, Z.; Testoff, T. T.; Wang, T.; Yan, X.; Li, W.; Liu, D.; Wang, L.; Zhou, X. *Anal. Chim. Acta* **2021**, *1153*, 338278.
(30) Zheng, Y.; Chen, Y.; Cao, Y.; Huang, F.; Guo, Y.; Zhu, X. *ACS Mater. Lett.* **2022**, *4*, 882.
(31) Liu, M.; Zong, J.; Wang, L.; Liu, D.; Wang, T.; Hu, W. *Adv. Opt. Mater.* **2022**, 2201684.
(32) Zhao, M.; Wei, Q.; Zhang, J.; Li, W.; Wang, Z.; Du, S.; Xue, Q.; Xie, G.; Ge, Z. *Org. Electronics* **2022**, *100*, 106365.
(33) Zhang, Y.; Mollick, S.; Tricarico, M.; Ye, J.; Sherman, D. A.; Tan, J.-C. *ACS Sens.* **2022**, *7*, 2338.
(34) Muleta, D. Y.; Song, J.; Feng, W.; Wu, R.; Zhou, X.; Li, W.; Wang, L.; Liu, D.; Wang, T.; Hu, W. *J. Mater. Chem. C* **2021**, *9*, 5093.
(35) Zhang, J.; Lan, T.; Lu, Y. *Annu. Rev. Anal. Chem.* **2022**, *15*, 151.
(36) Wang, Y.; Wang, X.; Ma, W.; Lu, R.; Zhou, W.; Gao, H. *Chemosensors* **2022**, *10*, 399.
(37) Wang, T.; Weerasinghe, K. C.; Sun, H.; Hu, X.; Lu, T.; Liu, D.; Hu, W.; Li, W.; Zhou, X.; Wang, L. *J. Phys. Chem. C* **2016**, *120*, 11338.
(38) Song, J.; Muleta, D. Y.; Feng, W.; Song, Y.; Zhou, X.; Li, W.; Wang, L.; Liu, D.; Wang, T.; Hu, W. *Dyes Pigm.* **2021**, *193*, 109501.
(39) Wang, T.; Liu, M.; Gao, C.; Song, Y.; Wang, L.; Liu, D.; Wang, T.; Hu, W. *Dyes Pigm.* **2022**, *207*, 110734.
(40) Wang, T.; Liu, M.; Feng, W.; Cao, R.; Sun, Y.; Wang, L.; Liu, D.; Wang, Y.; Wang, T.; Hu, W. *Adv. Opt. Mater.* **2023**, 2202613.
(41) Geng, Y.; Zhang, G.; Chen, Y.; Peng, Y.; Wang, X.; Wang, Z. *Anal. Chem.* **2022**, *94*, 1813.
(42) Alkhamis, O.; Canoura, J.; Bukhryakov, K. V.; Tarifa, A.; DeCaprio, A. P.; Xiao, Y. *Angew. Chem. Int. Ed.* **2022**, *61*, e202112305.
(43) Tian, X.; Murfin, L. C.; Wu, L.; Lewis, S. E.; James, T. D. *Chem. Sci.* **2021**, *12*, 3406.
(44) Shin, Y.-H.; Gutierrez-Wing, M. T.; Choi, J.-W. *J. Electrochem. Soc.* **2021**, *168*, 017502.
(45) S., K.; Sam, B.; George, L.; N, S. Y.; Varghese, A. *J. Fluoresc.* **2021**, *31*, 1251.
(46) Fang, T.; Elsen, F.; Vogeley, N.; Wang, D. *ACS Photonics* **2021**, *8*, 3448.
(47) Zhang, Q.; Wang, W.; Huang, S.; Yu, S.; Tan, T.; Zhang, J.-R.; Zhu, J.-J. *Chem. Sci.* **2020**, *11*, 1948.
(48) Liu, R.; McConnell, E. M.; Li, J.; Li, Y. *J. Mater. Chem. B* **2020**, *8*, 3213.
(49) Zhang, R.; Niu, G.; Li, X.; Guo, L.; Zhang, H.; Yang, R.; Chen, Y.; Yu, X.; Tang, B. Z. *Chem. Sci.* **2019**, *10*, 1994.
(50) Xiao, M.; Lai, W.; Man, T.; Chang, B.; Li, L.; Chandrasekaran, A. R.; Pei, H. *Chem. Rev.* **2019**, *119*, 11631.
(51) Strakova, K.; Assies, L.; Goujon, A.; Piazzolla, F.; Humeniuk, H. V.; Matile, S. *Chem. Rev.* **2019**, *119*, 10977.
(52) Han, J.; Feng, W.; Muleta, D. Y.; Bridgmohan, C. N.; Dang, Y.; Xie, G.; Zhang, H.; Zhou, X.; Li, W.; Wang, L.; Liu, D.; Dang, Y.; Wang, T.; Hu, W. *Adv. Funct. Mater.* **2019**, *29*, 1902503.
(53) Peng, L.; Xu, S.; Zheng, X.; Cheng, X.; Zhang, R.; Liu, J.; Liu, B.; Tong, A. *Anal. Chem.* **2017**, *89*, 3162.
(54) Du, Y.; Dong, S. *Anal. Chem.* **2017**, *89*, 189.
(55) Sumithra, M.; Sundaraganesan, N.; Rajesh, R.; Vetrivelan, V.; Ilangovan, V.; Javed, S.; Muthu, S. *Chem. Phys. Impact* **2023**, *6*, 100145.
(56) Manian, A.; Hudson, R. J.; Ramkissoon, P.; Smith, T. A.; Russo, S. P. *J. Chem. Theory Comput.* **2023**, *19*, 271.
(57) Zhou, X.; Liu, D.; Wang, T.; Hu, X.; Guo, J.; Weerasinghe, K. C.; Wang, L.; Li, W. *J. Photochem. Photobiol. A: Chem.* **2014**, *274*, 57.
(58) Zhang, N.; Yang, L.; Li, W.; Zhu, J.; Chi, K.; Chang, D.; Qiao, Y.; Wang, T.; Zhao, Y.; Lu, X.; Liu, Y. *J. Am. Chem. Soc.* **2022**, *144*, 21521.

(59) Zeng, L.; Huang, L.; Han, J.; Han, G. *Acc. Chem. Res.* **2022**, *55*, 2604.
(60) Sotome, H.; Koga, M.; Sawada, T.; Miyasaka, H. *Phys. Chem. Chem. Phys.* **2022**, *24*, 14187.
(61) Walkup, L. L.; Weerasinghe, K. C.; Tao, M.; Zhou, X.; Zhang, M.; Liu, D.; Wang, L. *J. Phys. Chem. C* **2010**, *114*, 19521.
(62) Wang, T.; Zhao, C.; Zhang, L.; Lu, T.; Sun, H.; Bridgmohan, C. N.; Weerasinghe, K. C.; Liu, D.; Hu, W.; Li, W.; Zhou, X.; Wang, L. *J. Phys. Chem. C* **2016**, *120*, 25263.
(63) Sharif, O. F. A.; Nhari, L. M.; El-Shishtawy, R. M.; Zayeda, M. E. M.; Asiri, A. M. *RSC Adv.* **2022**, *12*, 19270.
(64) Rauf, A.; Naeem, M.; Bukhari, S. U. *Int. J. Quantum Chem.* **2022**, *122*, e26851.
(65) Wang, T.; Weerasinghe, K. C.; Ubaldo, P. C.; Liu, D.; Li, W.; Zhou, X.; Wang, L. *Chem. Phys. Lett.* **2015**, *618*, 142.
(66) Oruganti, B.; Wang, J.; Durbeej, B. *J. Org. Chem.* **2022**, *87*, 11565.
(67) Nicksonsebastin, D.; Pounraj, P.; Prasath, M. *J. Mol. Model.* **2022**, *28*, 102.
(68) Nagaraju, N.; Kushavah, D.; Kumar, S.; Ray, R.; Gambhir, D.; Ghosh, S.; Pal, S. K. *Phys. Chem. Chem. Phys.* **2022**, *24*, 3303.
(69) Sun, H.; Li, P.; Liu, D.; Wang, T.; Li, W.; Hu, W.; Wang, L.; Zhou, X. *J. Photochem. Photobiol. A: Chem.* **2019**, *368*, 233.
(70) Loong, H.; Zhou, J.; Jiang, N.; Feng, Y.; Xie, G.; Liu, L.; Xie, Z. *J. Phys. Chem. B* **2022**, *126*, 2441.
(71) Yang, J.; Liu, D.; Lu, T.; Sun, H.; Li, W.; Testoff, T. T.; Zhou, X.; Wang, L. *Int. J. Quantum Chem.* **2020**, *120*, e26355.
(72) Weerasinghe, K. C.; Wang, T.; Zhuang, J.; Sun, H.; Liu, D.; Li, W.; Hu, W.; Zhou, X.; Wang, L. *Chem. Phys. Impact* **2022**, *4*, 100062.
(73) Wang, R.; Gong, K.; Liu, R.; Liu, D.; Li, W.; Wang, L.; Zhou, X. *J. Porphyrins Phthalocyanines* **2022**, *26*, 469.
(74) Feng, W.; Wang, T.; Testoff, T. T.; Bridgmohan, C. N.; Zhao, C.; Sun, H.; Hu, W.; Li, W.; Liu, D.; Wang, L.; Zhou, X. *Spectrochim. Acta. Part A* **2020**, *229*, 118016.
(75) Weerasinghe, K. C.; Wang, T.; Zhuang, J.; Liu, D.; Li, W.; Zhou, X.; Wang, L. *Comput. Mater. Sci.* **2017**, *126*, 244.
(76) Liraz, D.; Tesslera, N. *Chem. Phys. Rev.* **2022**, *3*, 031305.
(77) Ghadwal, R. S. *Acc. Chem. Res.* **2022**, *55*, 457.
(78) Dorofeeva, O. V.; Andreychev, V. V. *J. Phys. Chem. A* **2022**, *126*, 8315.
(79) Singh, A.; Humeniuk, A.; Roehr, M. I. S. *Phys. Chem. Chem. Phys.* **2021**, *23*, 16525.
(80) Shibasaki, Y.; Suenobu, T.; Nakagawa, T.; Katoh, R. *J. Phys. Chem. A* **2021**, *125*, 1359.
(81) Rajasekar, M. *J. Mol. Struct.* **2021**, *1224*, 129085.
(82) Pujari, S. R.; Nagore, P. B.; Ghoti, A. J.; Mane, K. G. *J. Fluoresc.* **2021**, *31*, 259.
(83) Price, J.; Balonova, B.; Blight, B. A.; Eisler, S. *Chem. Sci.* **2021**, *12*, 12092.
(84) Kiss, F. L.; Corbet, B. P.; Simeth, N. A.; Feringa, B. L.; Crespi, S. *Photochem. Photobiol. Sci.* **2021**, *20*, 927.
(85) Kandregula, G. R.; Mandal, S.; Mirle, C.; Ramanujam, K. *J. Photochem. Photobiol. A: Chem.* **2021**, *419*, 113447.
(86) Hall, C. L.; Andrusenko, I.; Potticary, J.; Gao, S.; Liu, X.; Schmidt, W.; Marom, N.; Mugnaioli, E.; Gemmi, M.; Hall, S. R. *ChemPhysChem* **2021**, *22*, 1631.
(87) Guo, S.; Dai, W.; Chen, X.; Lei, Y.; Shi, J.; Tong, B.; Cai, Z.; Dong, Y. *ACS Materials Lett.* **2021**, *3*, 379−397.
(88) Gong, Y.; Hou, G. L.; Bi, X.; Kuthirummal, N.; Teklu, A. A.; Koenemann, J.; Harris, N.; Wei, P.; Devera, K.; Hu, M. *J. Phys. Chem. A* **2021**, *125*, 1870.
(89) Dinleyici, M.; Al-Khateeb, B.; Abourajab, A.; Uzun, D.; Koyuncu, S.; Icil, H. *J. Photochem. Photobiol. A: Chem.* **2021**, *421*, 113525.

(90) Ye, C.; Gray, V.; Kushwaha, K.; Kumar Singh, S.; Erhart, P.; Boerjesson, K. *Phys. Chem. Chem. Phys.* **2020**, *22*, 1715.
(91) Valiev, R. R.; Baryshnikov, G. V.; Nasibullin, R. T.; Sundholm, D.; Ågren, H. *J. Phys. Chem. C* **2020**, *124*, 21027.
(92) Pearce, N.; Davies, E. S.; Champness, N. R. *Dyes Pigm.* **2020**, *183*, 108735.
(93) Liu, S.; Wang, X.; Liu, H.; Xiao, Z.; Zhou, C.; Chen, Y.; Li, X. *J. Phys. Chem. B* **2020**, *124*, 6389.
(94) Li, T.; Li, F.; Altuzarra, C.; Classen, A.; Agarwal, G. S. *Appl. Phys. Lett.* **2020**, *116*, 254001.
(95) Kiseleva, N.; Busko, D.; Richards, B. S.; Filatov, M. A.; Turshatov, A. *J. Phys. Chem. Lett.* **2020**, *11*, 6560.
(96) Muramatsu, K.; Okujima, T.; Mori, S.; Kikuchi, S.; Ando, S.; Okada, Y.; Takase, M.; Uno, H.; Kobayashi, N. *Org. Lett.* **2023**, *25*, 3049.
(97) Jozeliūnaitė, A.; Neniškis, A.; Bertran, A.; Bowen, A. M.; Valentin, M. D.; Raišys, S.; Baronas, P.; Kazlauskas, K.; Vilčiauskas, L.; Orentas, E. *J. Am. Chem. Soc.* **2023**, *145*, 455.
(98) Guo, W.; Ding, W.; Yao, Y.; Rajca, S.; Li, Q.; Jiang, H.; Rajca, A.; Wang, Y. *Org. Lett.* **2023**, *25*, 3972.
(99) Wu, Z.; Zhang, M.; Jiang, H.; Zhong, C.-J.; Chen, Y.; Wang, L. *Phys. Chem. Chem. Phys.* **2017**, *19*, 15444.
(100) Liu, J.; Li, X.; Zhang, L.; Liu, X.; Wang, X. *Carbon* **2022**, *188*, 453.
(101) Komatsubara, K.; Inagaki, Y.; Setaka, W. *J. Org. Chem.* **2022**, *87*, 12783.
(102) Lu, J.; Aydin, C.; Browning, N. D.; Wang, L.; Gates, B. C. *Catal. Lett.* **2012**, *142*, 1445.
(103) Miao, B.; Wu, Z.-P.; Xu, H.; Zhang, M.; Chen, Y.; Wang, L. *Comput. Mater. Sci.* **2019**, *156*, 175.
(104) Wang, Y.-H.; Wang, L.-T.; Yao, Z.-Z.; Yin, J.-J.; Huang, Z.-B.; Yuan, P.-Q.; Yuan, W.-K. *Chem. Eng. Sci.* **2021**, *232*, 116342.
(105) Wu, R.; Wang, L. *Chem. Phys. Lett.* **2017**, *678*, 196.
(106) Miao, B.; Wu, Z.; Xu, H.; Zhang, M.; Chen, Y.; Wang, L. *Chem. Phys. Lett.* **2017**, *688*, 92.
(107) Tian, D.; Shi, G.; Fan, M.; Guo, X.; Yuan, Y.; Wu, S.; Liu, J.; Zhang, J.; Xing, S.; Zhu, B. *Org. Lett.* **2021**, *23*, 8163.
(108) Xu, H.; Miao, B.; Zhang, M.; Chen, Y.; Wang, L. *Phys. Chem. Chem. Phys.* **2017**, *19*, 26210.
(109) Rawat, N.; Sinha, A.; Prasannan, D.; Ravikanth, M. *J. Org. Chem.* **2021**, *86*, 6665.
(110) Wu, R.; Wang, L. *J. Phys. Chem. C* **2020**, *124*, 26953.
(111) Wang, L.; Ore, R. M.; Jayamaha, P. K.; Wu, Z.-P.; Zhong, C.-J. *Faraday Discuss.* **2023**, *242*, 429.
(112) Ohtomo, Y.; Ishiwata, K.; Hashimoto, S.; Kuroiwa, T.; Tahara, K. *J. Org. Chem.* **2021**, *86*, 13198.
(113) Koner, A.; Sergeieva, T.; Morgenstern, B.; Andrada, D. M. *Inorg. Chem.* **2021**, *60*, 14202.
(114) Jun Zhu, Y. H.; Ni, Y.; Wu, S.; Zhang, Q.; Jiao, T.; Li, Z.; Wu, J. *J. Am. Chem. Soc.* **2021**, *143*, 14314.
(115) Wu, C.; Wang, L.; Xiao, Z.; Li, G.; Wang, L. *Phys. Chem. Chem. Phys.* **2020**, *22*, 724.
(116) Chen, P.-Y.; Liu, Y.-C.; Hung, H.-Y.; Pan, M.-L.; Wei, Y.-C.; Kuo, T.-C.; Cheng, M.-J.; Chou, P.-T.; Chiang, M.-H.; Wu, Y.-T. *Org. Lett.* **2021**, *23*, 8794.
(117) Whittemore, T. J.; Xue, C.; Huang, J.; Gallucci, J. C.; Turro, C. *Nat. Chem.* **2020**, *12*, 180.
(118) Watanabe, H.; Takemoto, M.; Adachi, K.; Okuda, Y.; Dakegata, A.; Fukuyama, T.; Ryu, I.; Wakamatsu, K.; Orita, A. *Chem. Lett.* **2020**, *49*, 409.
(119) Wu, R.; Sun, K.; Chen, Y.; Zhang, M.; Wang, L. *Surf. Sci.* **2021**, *703*, 121742.
(120) Wu, R.; Wang, L. *Chem. Phys. Impact* **2021**, *3*, 100040.
(121) Wu, R.; Wang, L. *ChemPhysChem* **2022**, *23*, e202200132.
(122) Michael W. Gribble, J.; Liu, R. Y.; Buchwald, S. L. *J. Am. Chem. Soc.* **2020**, *142*, 11252.

(123) Ma, X.; Maier, J.; Wenzel, M.; Friedrich, A.; Steffen, A.; Marder, T. B.; Mitric, R.; Brixner, T. *Chem. Sci.* **2020**, *11*, 9198.
(124) Wu, R.; Wang, L. *Comput. Mater. Sci.* **2021**, *196*, 110514.
(125) Wu, R.; Wiegand, K. R.; Wang, L. *J. Chem. Phys.* **2021**, *154*, 054705.
(126) Wu, C.; Xiao, Z.; Wang, L.; Li, G.; Zhang, X.; Wang, L. *Catal. Sci. Technol.* **2021**, *11*, 1965.
(127) Wu, R.; Wiegand, K. R.; Ge, L.; Wang, L. *J. Phys. Chem. C* **2021**, *125*, 14275.
(128) Wu, R.; Wang, L. *J. Phys. Chem. C* **2022**, *126*, 21650.
(129) Hwang, S.-H.; Choi, T.-L. *Org. Lett.* **2020**, *22*, 2935.
(130) Wu, R.; Wang, L. *Phys. Chem. Chem. Phys.* **2023**, *25*, 2190.
(131) Wu, C.; Wang, L.; Xiao, Z.; Li, G.; Wang, L. *Chem. Phys. Lett.* **2020**, *746*, 137229.
(132) Achelle, S.; Rodríguez-López, J.; Larbani, M.; Plaza-Pedroche, R.; Guen, F. R.-l. *Molecules* **2019**, *24*, 1742.
(133) Zhao, C.; Wang, T.; Li, D.; Lu, T.; Liu, D.; Meng, Q.; Zhang, Q.; Li, F.; Li, W.; Hu, W.; Wang, L.; Zhou, X. *Dye Pigm.* **2017**, *137*, 256.
(134) Zhao, J.; Zheng, X. *Front. Chem.* **2022**, *9*, 808957.
(135) Testoff, T. T.; Aikawa, T.; Tsung, E.; Lesko, E.; Wang, L. *Chem. Phys.* **2022**, *562*, 111641.
(136) Wei, H.; Min, J.; Wang, Y.; Shen, Y.; Du, Y.; Su, R.; Qi, W. *J. Mater. Chem. B* **2022**, *10*, 9334.
(137) Wang, L.; Liu, Y.-L.; Li, Q.-J.; Chen, S.-H.; He, D.; Wang, M.-S. *J. Phys. Chem. A* **2022**, *126*, 870.
(138) Waly, S. M.; Karlsson, J. K. G.; Waddell, P. G.; Benniston, A. C.; Harriman, A. *J. Phys. Chem. A* **2022**, *126*, 1530−1541.
(139) Sun, S.; Conrad-Burton, F. S.; Liu, Y.; Ng, F.; Steigerwald, M.; Zhu, X.; Nuckolls, C. *J. Phys. Chem. A* **2022**, *126*, 7559.
(140) Roosta, S.; Ghalami, F.; Elstner, M.; Xie, W. *J. Chem. Theory Comput.* **2022**, *18*, 1264.
(141) Parida, S.; Patra, S. K.; Mishra, S. *ChemPhysChem* **2022**, *23*, e202200361.
(142) Murai, M.; Abe, M.; Ogi, S.; Yamaguchi, S. *J. Am. Chem. Soc.* **2022**, *144*, 20385.
(143) Liu, R.; Liu, D.; Meng, F.; Li, W.; Wang, L.; Zhou, X. *Dyes Pigm.* **2021**, *187*, 109135.
(144) Xu, F.; Gong, K.; Fan, W.; Liu, D.; Li, W.; Wang, L.; Zhou, X. *ACS Appl. Energy Mater.* **2022**, *5*, 13780.
(145) Hai, T.; Feng, Z.; Sun, Y.; Wong, W.-Y.; Liang, Y.; Zhang, Q.; Lei, Y. *ACS Nano* **2022**, *16*, 3290.
(146) Bernhardt, R.; Manrho, M.; Zablocki, J.; Rieland, L.; Lützen, A.; Schiek, M.; Meerholz, K.; Zhu, J.; Jansen, T. L. C.; Knoester, J.; Loosdrecht, P. H. M. v. *J. Am. Chem. Soc.* **2022**, *144*, 19372−19381.
(147) Afraj, S. N.; Lin, C.-C.; Velusamy, A.; Cho, C.-H.; Liu, H.-Y.; Chen, J.; Lee, G.-H.; Fu, J.-C.; Ni, J.-S.; Tung, S.-H.; Yau, S.; Liu, C.-L.; Chen, M.-C.; Facchetti, A. *Adv. Funct. Mater.* **2022**, *32*, 2200880.
(148) Zhang, P.-F.; Zeng, J.-C.; Zhuang, F.-D.; Zhao, K.-X.; Sun, Z.-H.; Yao, Z.-F.; Lu, Y.; Wang, X.-Y.; Wang, J.-Y.; Pei, J. *Angew. Chem., Int. Ed.* **2021**, *60*, 23313.
(149) Wu, R.; Wang, Y.; Zhu, Z.; Yu, C.; Li, H.; Li, B.; Dong, S. *ACS Appl. Mater. Interfaces* **2021**, *13*, 9482.
(150) Wang, Y.; Qin, W. *Org. Electron.* **2021**, *92*, 106103.
(151) Ni, W.; Sun, L.; Gurzadyan, G. G. *Sci. Rep.* **2021**, *11*, 5220.
(152) Liu, X.; Pan, Y.; Lei, Y.; Liu, N.; Dai, W.; Liu, M.; Cai, Z.; Wu, H.; Huang, X.; Dong, Y. *J. Phys. Chem. Lett.* **2021**, *12*, 7357−7364.
(153) Li, Q.-Y.; Yao, Z.-F.; Wang, J.-Y.; Pei, J. *Rep. Prog. Phys.* **2021**, *84*, 076601.
(154) Kundu, S.; Makri, N. *J. Chem. Phys.* **2021**, *154*, 114301.

(155) Dixit, S. J. N.; Awasthi, A. A.; Chandrakumar, K. R. S.; Manna, B.; Agarwal, N. *J. Phys. Chem. C* **2021**, *125*, 20405.
(156) Chen, Z.; Li, W.; Zhang, Y.; Wang, Z.; Zhu, W.; Zeng, M.; Li, Y. *J. Phys. Chem. Lett.* **2021**, *12*, 9783.
(157) Zhao, W.; He, Z.; Tang, B. Z. *Nat. Rev. Mater.* **2020**, *5*, 869.
(158) Sabuzi, F.; Stefanelli, M.; Monti, D.; Conte, V.; Galloni, P. *Molecules* **2020**, *25*, 133.
(159) Pigulski, B.; Ximenis, M.; Shoyama, K.; Wuerthner, F. *Org. Chem. Front.* **2020**, *7*, 2925.
(160) Manna, B.; Palit, D. K. *J. Phys. Chem. C* **2020**, *124*, 24470.
(161) Chang, M.; Meng, L.; Wang, Y.; Ke, X.; Yi, Y.-Q.-Q.; Zheng, N.; Zheng, W.; Xie, Z.; Zhang, M.; Yi, Y.; Zhang, H.; Wan, X.; Li, C.; Chen, Y. *Chem. Mater.* **2020**, *32*, 2593.
(162) Zhou, R.; Jiang, Z.; Yang, C.; Yu, J.; Feng, J.; Adil, M. A.; Deng, D.; Zou, W.; Zhang, J.; Lu, K.; Ma, W.; Gao, F.; Wei, Z. *Nat. Commun.* **2019**, *10*, 5393.
(163) Ma, H.; Yu, H.; Peng, Q.; An, Z.; Wang, D.; Shuai, Z. *J. Phys. Chem. Lett.* **2019**, *10*, 6948.
(164) Hestand, N. J.; Spano, F. C. *Chem. Rev.* **2018**, *118*, 7069.
(165) Ang, S. T.; Pal, A.; Manzhos, S. *J. Chem. Phys.* **2018**, *149*, 044114.
(166) Eastham, N. D.; Dudnik, A. S.; Aldrich, T. J.; Manley, E. F.; Fauvell, T. J.; Hartnett, P. E.; Wasielewski, M. R.; Chen, L. X.; Melkonyan, F. S.; Facchetti, A.; Chang, R. P. H.; Marks, T. J. *Chem. Mater.* **2017**, *29*, 4432.
(167) Zhang, X.; Jie, J.; Deng, W.; Shang, Q.; Wang, J.; Wang, H.; Chen, X.; Zhang, X. *Adv. Mater.* **2016**, *28*, 2475.
(168) Würthner, F.; Saha-Möller, C. R.; Fimmel, B.; Ogi, S.; Leowanawat, P.; Schmidt, D. *Chem. Rev.* **2016**, *116*, 962.
(169) Testoff, T. T.; Wang, L. *ChemRxiv* **2023**, 10.26434/chemrxiv.
(170) Xu, T.; Wang, W.; Yin, S. *J. Chem. Theory Comput.* **2018**, *14*, 3728.
(171) Ponder, J. W.; Wu, C.; Ren, P.; Pande, V. S.; Chodera, J. D.; Schnieders, M. J.; Haque, I.; Mobley, D. L.; Lambrecht, D. S.; Distasio, R. A.; Head-Gordon, M.; Clark, G. N. I.; Johnson, M. E.; Head-Gordon, T. *J. Phys. Chem. B* **2010**, *114*, 2549.
(172) Ren, P.; Ponder, J. W. *J. Comput. Chem.* **2002**, *23*, 1497.